Pressure-induced anomalies and structural instability in compressed β-Sb2O3

Journal:	*Physical Chemistry Chemical Physics*
Manuscript ID	CP-ART-01-2018-000084.R2
Article Type:	Paper
Date Submitted by the Author:	07-Apr-2018

Complete List of Authors:	Zou, Yongtao; Southern University of Science and Technology, Zhang, Wei; Southwest University of Science and Technology, Li, Xuefei; Mineral Physics Institute, State University of New York at Stony Brook, Ma, Maining; University of the Chinese Academy of Sciences Li, Xingao; Nanjing University of Posts and Telecommunications, School of Science Wang, Chun-Hai; Southern University of Science and Technology He, Bin; Southern University of Science and Technology wang, shanmin; Southern University of Science & Technology, Department of Physics Chen, Zhiqiang; Center for High Pressure Science and Technology Advanced Research (HPSTAR) Zhao, Yusheng; Southern University of Science & Technology, Department of Physics Li, Baosheng; Mineral Physics Institute, State University of New York at Stony Brook, ;

Pressure-induced anomalies and structural instability in compressed β-Sb_2O_3

Yongtao Zou,[a,b,*] Wei Zhang,[c] Xuefei Li,[d] Maining Ma,[e] Xing'ao Li,[f] Chun-Hai Wang,[a] Bin He,[a] Shanmin Wang,[a] Zhiqiang Chen,[b,g] Yusheng Zhao,[a,*] and Baosheng Li[b,*]

[a]*Academy for Advanced Interdisciplinary Studies, and Department of Physics, Southern University of Science and Technology, Shenzhen, 518055, China*

[b]*Mineral Physics Institute, State University of New York, Stony Brook, N.Y. 11794, United States*

[c]*School of Science, Southwest University of Science and Technology, Mianyang, Sichuan 610064, China*

[d]*Key Laboratory of Functional Materials Physics and Chemistry of the Ministry of Education, Jilin Normal University, Siping 136000, China*

[e]*Key Laboratory of Computational Geodynamics of Chinese Academy of Sciences, University of Chinese Academy of Sciences, Beijing 100049, China*

[f]*School of Science, Nanjing University of Posts and Telecommunications, Nanjing 210046, China*

[g]*Center for High Pressure Science and Technology Advanced Research (HPSTAR), Shanghai 201203, China*

*E-mail: zouyt@sustc.edu.cn; zhaoys@sustc.edu.cn; baosheng.li@stonybrook.edu

Abstract

Here, we report a high-pressure study of orthorhombic structured β-Sb_2O_3 (valentinite) by the combination of synchrotron *in situ* x-ray diffraction and first-principles theoretical calculations at pressures up to 40.5 GPa. Our results reveal that the metastable β-Sb_2O_3 undergoes an isostructural phase transition at high pressure, yielding a distorted β phase at 7~15 GPa through symmetry breaking and structural distortion as inferred from our XRD analyses and DFT theoretical calculations where pressure-induced elasticity softening is observed at pressures of 7~15 GPa. At pressures higher than 15 GPa, a new high-pressure monoclinic phase is discovered from the current synchrotron x-ray diffraction data. Upon further compression up to ~33 GPa, the monoclinic Sb_2O_3 starts to lose its

long-range order and forms an amorphous component coexisting with the monoclinic one. To further explore the structural instability and understand the origin of pressure-induced phase transitions in β-Sb_2O_3 upon compression, we have performed first-principles calculations to track the evolution of its phonon velocities, density of states and phonon dispersion curves under high pressure. Our results may play an important role in determining the local structures as well as their structural relationship among sesquioxides.

I. Introduction

Nowadays, antimony sesquioxide, like the As_2O_3 and Bi_2O_3 XV group compounds, has attracted great interest owing to its outstanding mechanical, chemical and electronic properties, and has been widely used in industry as flame retardants for ceramics and fibers, photo-catalyses, anode materials for Li-ion batteries, as well as in the manufacture of semiconductors and glassy/optical devices.[1-6] To date, the known solid phases of Sb_2O_3 consist of an amorphous and four crystalline structures, namely senarmonite (α-Sb_2O_3),[7,8] valentinite (β-Sb_2O_3),[8] γ-Sb_2O_3[9] and a layered tetragonal phase.[10] It is known that α-Sb_2O_3 (senarmonite) has a cubic structure (space group *Fd-3m*) composed of spherical-top Sb_4O_6 "dimers" that form damantanoid cages, and it remains the cubic α phase at temperatures below ~843 K at ambient pressure.[7] The metastable orthorhombic β-Sb_2O_3 (space group: *Pccn*) consists of chains of four-membered rings formed by SbO_3 pyramids, which can be thermodynamically stable up to 7 GPa at 473 K, or becomes stable at temperatures ranging from ~843 K to its melting point at ambient pressure.[8,9] Recently, a newly discovered tetragonal phase of Sb_2O_3, as identified by high-pressure x-ray diffraction experiments, has been found to be stable at pressures of 15~20 GPa.[10]

It is proposed that the structures of sesquioxides of late group XV elements are quite different from those of sesquioxides of simple metals. For example, c-As_2O_3 arsenolite has a cubic structure similar to α-Sb_2O_3, and β-Sb_2O_3 is isostructural to ε-Bi_2O_3.[3,11,12] Interestingly, recent theoretical

calculations show that many structures such as α-Sb_2O_3 and β-Sb_2O_3, could be derived from a defective fluorite structure through symmetry breakings and local distortions.[3,13] In these sesquioxides, the presence of a lone electron pair in the metal atoms was proposed to play a central role in the determination of the local atomic arrangement.[3] High-pressure can efficiently tune the atomic distances and arrangements, and thus may enable us to explore the correlations between these structural models. Previous studies have presented a number of pressure-induced structural phase transitions and/or amorphization in sesquioxides of late group XV elements such as Bi_2O_3, Sb_2O_3 and As_2O_3.[2,3,13,14] As reported in these studies, arsenolite (c-As_2O_3) and monoclinic α-Bi_2O_3 underwent crystalline-to-amorphous phase transitions above 15 and 20 GPa, respectively.[3, 13] For α-Sb_2O_3, high-pressure x-ray diffraction (XRD) and Raman experiments combined with *ab initio* calculations demonstrated that two isostructural phase transitions occurred at pressures of 3.5 and 10 GPa, respectively, and it was suggested to further transform into a layered tetragonal structure at pressures above 25 GPa.[10] For β-Sb_2O_3, a pressure-induced structural phase transition at pressures between 8.6~15 GPa was proposed by Raman measurements in a diamond-anvil-cell,[2] however, this new phase proposed by Geng *et al.*[2] and Pereira *et al.*[4] has never been verified experimentally by x-ray diffraction study. In this study, we presented structure and stability studies on β-Sb_2O_3 at high pressure by *in situ* x-ray diffraction and first-principles calculations.

II. Experimental and theoretical methods

Commercial β-Sb_2O_3 powder was used as starting materials in the current experiments. *In situ* high-resolution angle-dispersive x-ray experiments were performed in diamond-anvil-cells (DACs) with 300-μm culets size at the X17C beamline of National Synchrotron Light Source, Brookhaven National Laboratory. The x-ray wavelength was ~0.4066 Å. Stainless T301 steel plates with an initial thickness of 250 μm were used as gaskets. The center of the plate was pre-indented to a thickness of

~60 μm, and a hole of ~150 μm in diameter was drilled by an electric discharge machine.[15] The starting material of β-Sb_2O_3 powder, a tiny ruby ball, and methanol-ethanol pressure medium (4:1) were loaded into the hole in the gasket. Cell-pressures were determined by measuring the shift of fluorescence peaks of ruby.[16] X-ray diffraction patterns were collected using an online detector with a collecting time of 5~10 min at certain pressure. Two-dimensional x-ray diffraction patterns were analyzed by integrating intensity as a function of 2θ using the Fit2D program to derive conventional, one-dimensional profiles.[17]

Our first-principles calculations were performed using the CASTEP code based on density functional theory (DFT) using Vanderbilt-type ultrasoft pseudo potentials and a plane-wave expansion of the wave functions.[18] The local density approximation (LDA) and the generalized gradient approximation (GGA) were employed for the determination of the exchange and correlation potentials for electron-electron interactions. The valence configurations are $5s^25p^3$ for Sb and $2s^22p^4$ for O, respectively. When calculating elastic/electronic properties, the plane wave energy cutoff was set to 700 eV, and the crystal reciprocal-lattice and integration over the first Brillouin zone were performed using 6×2×6 Monkhorst-Pack k-points mesh.[19] For the calculation of phonon dispersion spectra, we used the linear response method within the density functional perturbation theory (DFPT), and norm-conserving pseudo potentials were used to describe ion-electron interactions with energy cutoff of 800 eV and Monkhorst-Pack k-points mesh of 9×3×9. During our first-principles calculations, the difference in total energy is minimized to 10^{-6} eV/atom, the maximum ionic Hellmann-Feynman force is converged to less than 0.01 eV/Å, and the total stress tensor is reduced to an order of 0.02 GPa by using the finite basis-set corrections.

III. Results and discussion

As shown in Fig. 1(a), the as-prepared Sb_2O_3 powder has an orthorhombic structure (valentinite)

at ambient conditions, which belongs to the space group No. 56 (*Pccn*). The crystal structure of valentinite β-Sb_2O_3 is shown in Fig. 1(a) as an inset, where each Sb atom is surrounded by five oxygen atoms, and two different O atoms are surrounded by four and three Sb atoms, respectively. It consists of chains of four-membered rings formed by SbO_3 pyramids. For comparison, a representative x-ray diffraction pattern of Sb_2O_3 upon compression at 8.8 GPa and room temperature is shown in Fig. 1(b), indicating a distorted orthorhombic structure (also called distorted β phase) as referred from the x-ray peaks. With further compression, the distorted orthorhombic Sb_2O_3 becomes more distorted, and the β angle between the *a* and *c* axes becomes larger than 90°, transforming into a monoclinic structure. A representative x-ray diffraction pattern of the new monoclinic Sb_2O_3 phase at 21.3 GPa and 300 K is shown in Fig. 1(c). Clearly, this new monoclinic-phase occurred at pressures higher than ~15 GPa is different from a layered tetragonal structure formed above 25 GPa.[10] For good understanding, crystal structure including lattice parameters, unit-cell volumes and atomic positions of the newly discovered monoclinic-Sb_2O_3 phase at 21.3 GPa and 300 K is summarized in Table 1, in comparison with those for Sb_2O_3 polymorphs.

To probe the structural evolution of β-Sb_2O_3 at high pressure, a comparison of x-ray diffraction patterns for β-Sb_2O_3 upon compression up to ~40.5 GPa and during decompression is shown in Fig. 2(a). For clarity, the enlarged x-ray diffraction patterns within 8.4~9.4° are shown in Fig. 2(b). It is found that the orthorhombic structure of β-Sb_2O_3 can be stable up to ~7 GPa at room temperature. With increasing pressure, an apparent splitting of a peak at ~8.92° in the x-ray diffraction pattern is observed which persists up to ~14.4 GPa, but the sample still adopts the orthorhombic structure. The spit peaks of (121), (040) and (012) as well as the shift of the typical peaks (labeled as blue asterisks in Fig. 2b) indicates that the structural distortion occurs upon compression. At pressures above ~15 GPa, the distorted β phase is found to further transform into a new monoclinic phase upon compression (see Fig. 1c). Upon further compression, the monoclinic Sb_2O_3 phase starts to lose its long-range order and

an amorphous component is observed at pressures higher than ~28.3 GPa, coexisting with the amorphous phase because of its sluggish amorphization (see an inset in Fig. 2a). During decompression to ambient conditions, the new monoclinic phase and amorphous component of Sb_2O_3 are found to transform back to the orthorhombic structured β-Sb_2O_3, indicating reversible pressure-induced phase transitions, as shown in the top-right panel of Fig. 2(a).

Fig. 3(a) shows unit-cell volumes (V) of β-Sb_2O_3 valentinite at hydrostatic conditions ($P \leqq 10$ GPa: before the solidification of methanol-ethanol pressure medium) from the present static-compression experiments, in comparison with our DFT theoretical predictions. Fitting the current experimental P-V data to the second-order Birch-Mürnaghan equation of state[15] (EOS) yielded $B_0 = 40.0 \pm 1.1$ GPa, $V_0 = 331.0 \pm 1.0$ Å^3 with $B' = 4.0$, where V_0, B_0, and B' are the unit-cell volume, isothermal bulk modulus, and its pressure derivative at ambient conditions, respectively. Our obtained bulk modulus ($B_0 = 40.0 \pm 1.1$ GPa) agrees well with our first-principles result of $B_0 = 42.1$ GPa. In contrast, the experimentally derived unit-cell volume ($V_0 = 331.0$ Å^3) is ~9% larger than our DFT calculations result. This difference between the experimental and theoretical unit-cell volume might originate from the overbinding of LDA,[20] as well as the effect of temperature.

Fig. 3(b) shows x-ray densities of Sb_2O_3 polymorphs as a function of pressure determined from the current x-ray diffraction measurements, together with the theoretical results for orthorhombic β-Sb_2O_3. Clearly, the density increases with pressures up to ~15 GPa with a very subtle discontinuity at ~7.5 GPa, which is different from the continuously theoretical values with pressures. This anomaly may be attributed to the isostructural phase transformation from the orthorhombic β-Sb_2O_3 phase to a distorted one. At pressures higher than ~15 GPa, however, a pronounced density decrease/drop is observed, which is attributed to the formation of a new monoclinic Sb_2O_3 phase. This new phase will coexist with the pressured-induced amorphous Sb_2O_3 component at even high pressures above ~28.3 GPa, persisting up to ~40.5 GPa (Fig. 2a).

To further explore the phase-transition-induced anomalies at high pressure, a representative x-ray diffraction (XRD) FWHM (full width at half maximum) pattern for (121) peak against pressures is shown in Fig. 3(c). It is found that the FWHM pattern exhibits an apparent drop at ~7.5 GPa, supporting a strong evidence for the pressure-induced phase transition from the orthorhombic structure to a distorted one (also see enlarged Fig. 2b and Fig. 3b). It is worth mentioning that the Sb_2O_3 material is very soft, which may be a good candidate for pressure medium and provide a nearly hydrostatic experimental condition, even above the solidification pressure of 10~11 GPa for methanol-ethanol (4:1) pressure medium. At higher pressure, an obvious discontinuity in FWHM is observed at ~15 GPa, which could not be due to the negligible nonhydrostatic condition or small stress existed in the sample, but the formation of a more distorted structure, namely the new monoclinic Sb_2O_3 phase, resulting in a pronounced density decrease/drop at pressures above ~15 GPa. To further confirm these distortion phase-transitions, *d*-spacings for typical x-ray peaks of (121), (040) and (012) as a function of pressure are shown in Fig. 3(c) as an inset. The tendency in *d*-spacings with pressures is consistent well with our x-ray FWHM analyses results. With further increase of pressures, the FWHM pattern exhibits a significant drop at ~33 GPa, which is attributed to stress relaxations caused by the monoclinic-to-amorphization phase transition upon compression. This stress is usually existing in an aggregate polycrystalline sample due to grain-to-grain contacts at high pressure.[21] To clearly know about the structural evolution and/or structural stability, pathways of the phase transformations in β-Sb_2O_3 upon compression are shown in Fig. 3(d).

To confirm the structural instability of β-Sb_2O_3 at high pressure, experimental lattice parameters (*a, b, c*) of Sb_2O_3 polymorphs upon compression are shown in Fig. 4(a). Clearly, the pronounced discontinuities at ~7.5 and ~15 GPa as discussed in the pressure dependence of the density (Fig. 3b), are also observed here, where the anomalies at ~7.5 and ~15 GPa are proposed to the isostructural phase-transition from β to a distorted-β phase, and the occurrence of a new monoclinic-Sb_2O_3 phase,

respectively. On the other hand, as shown in Fig. 4(b), the orthorhombic structured β-Sb_2O_3 becomes distorted with pressures and exhibits apparent slop changes in the lattice ratio of *a/c* from both our experimental observations and theoretical predictions. At even higher pressures above ~15 GPa in Fig. 4c, the β angles between the *a* and *c* axes becomes more and more distorted, resulting in the formation of a new monoclinic Sb_2O_3 phase upon compression.

To further probe the pressure-induced anomalies and structural instability in Sb_2O_3, phonon/acoustic velocities of the orthorhombic β-Sb_2O_3 under high pressure are predicted by first-principles calculations shown in Fig. 5(a). Clearly, our experimental exploration of the distorted orthorhombic-to-monoclinic phase-transition-induced anomaly at ~15 GPa (Figs. 1c, 3b, 3c and 4) is further supported by the currently predicted acoustic velocities in Fig. 5(a). By contrast, at the low pressure region, our experimentally observed discontinuity at ~7.5 GPa (Figs. 3b, 3c and 4) is also supported by the previous Raman spectroscopy measurements on β-Sb_2O_3 where new Raman peaks in the external lattice mode range occurred at pressures around 8.6~15 GPa which is proposed to the pressure-induced isostructural phase transition in β-Sb_2O_3 (Fig. 5b modified from Ref. 2). To explore dynamical instability of the orthorhombic β-Sb_2O_3 at high pressure, phonon dispersion curves at typical pressures of 7.0 and 7.5 GPa are shown in Figs. 5(c) and 5(d). With increasing pressure shown in Fig. 5(d), imaginary vibrational modes appear in the Brillouin zone, indicating that the orthorhombic β-Sb_2O_3 phase becomes dynamically unstable at pressures above 7.5 GPa, which further supports our experimental observations of the orthorhombic-to-distorted-β Sb_2O_3 phase transition at ~7.5 GPa upon compression.

Under high pressure, we have observed that the color of the Sb_2O_3 specimen evolved from white to red, then to yellow upon compression (the optical photographs are shown in the insets of Fig. 4b). Such dramatic changes in colors indicate possible phase transitions at high pressure and prompt us to study its electronic properties. To clearly clarify our observed pressure-induced anomalies and

structural instability/phase transitions of β-Sb_2O_3, electronic properties, total densities of states (TDOS) and partial densities of states (PDOS) for orthorhombic Sb_2O_3 at representative pressures have been calculated by first-principles, as shown in Fig. 6(a)-(c). It is found that β-Sb_2O_3 exhibits pronounced semiconducting bonding features with an obvious band gap at the Fermi level (E_F) at 0 GPa, originating mostly from the *5p* electrons of Sb and 2*p* electrons of O. At the lowermost valence band (below -8 eV), the DOS of β-Sb_2O_3 predominantly contains Sb 5*s* and HoweveO 2*p* states. r, at the topmost valence band (-8~0 eV), the valence-band maximum is mainly composed by Sb 5*p* and O 2*p* states with a minor contribution of Sb 5*s* states. Similar to the topmost valence band, the conduction band contains a peak comprising Sb 5*p* and O 2*p* states; however, there is also a minor contribution from the Sb 5*s* states. As shown in Fig. 6, our theoretically predicted band gap *Eg* decreases monotonically with increasing pressures, which agrees with our experimentally observed color changes in specimen from white to red at relatively low pressures within 7~10 GPa. Upon further compression, however, we find that our observed color is changing from the red to yellow at pressures above ~15 GPa which indicates an increase of band gap upon compression, in contrast to decreased *Eg* with pressures by theoretical calculations in Fig. 6(c) without consideration of electronic properties of new monoclinic phase. Therefore, the reason for the red-to-yellow color change at pressures above ~15 GPa is related to the formation of a new monoclinic-phase from the pressure-induced phase transition in distorted orthorhombic β-Sb_2O_3.

IV. Conclusions

In summary, we have investigated pressure-induced anomalies and structural instability of β-Sb_2O_3 (valentinite) by synchrotron *in situ* x-ray diffraction measurements and first-principles theoretical calculations up to 40.5 GPa. Our results reveal that the orthorhombic metastable β-Sb_2O_3 is subjected to isostructural phase transition at pressures of 7~15 GPa, yielding a distorted β phase

through symmetry breaking and local structural distortions as inferred from the current x-ray diffraction analyses, which is further supported by our DFT theoretical predictions. With the further increase of pressures, the distorted orthorhombic β structure becomes more and more distorted, and transforms into a new-monoclinic phase at pressures above ~15 GPa, then started to change into an amorphous component at ~28.3 GPa. This findings may provide important information for good understanding of the structural evolution/phase stability and elastic properties of Sb_2O_3 polymorphs for its use at extreme conditions.

Acknowledgements

This work is supported by Shenzhen Peacock Team Project (No. KQTD2016053019134356) and Guangdong Innovative & Entrepreneurial Research Team Program (No. 2016ZT06C279), and also supported by the NSF (EAR1524078) and DOE/NNSA (DE-NA0002907).

References

1 H. Bryngelsson, J. Eskhult, L. Nyholm, M. Herranen, O. Alm, K. Edström, *Chem. Mater.,* 2017, **19**, 1170.

2 A. Geng, L. Cao, C. Wan, Y. Ma, *Phys. Status Solidi C,* 2011, **8**, 1708.

3 A. Matsumoto, Y. Koyama, A. Togo, M. Choi, I. Tanaka, *Phys. Rev. B,* 2011, **83**, 214110.

4 A. L. J. Pereira, L. Gracia, D. Santamaria-Perez, R. Vilaplana, F. J. Manjón, D. Errandonea, M. Nalin, A. Beltrán, *Phys. Rev. B,* 2008, **85**, 174108.

5 M. Nalin, Y. Messaddeq, S. J. L. Ribeiro, M. Poulain, V. Briois, G. Brunklaus, C. Rosenhahn, B. D. Mosel, H. Eckert, *J. Mater. Chem.,* 2004, **14**, 3398.

6 E. L. Falcão Filho, C. A. C. Bosco, G. S. Maciel, C. B. De. Araújo, L. H. Acioli, *Appl. Phys. Lett.,* 2003, **83**, 1292.

7 C. Svensson, *Acta Crystallogr., Sect B,* 1975, **31**, 2016.

8 P. S. Gopalakrishnan, H. Manohar, *J. Solid State Chem.,* 1975, **15**, 61.

9 D. Orosel, R. E. Dinnebier, V. A. Blatov, M. Jansen, *Acta Crystallogr., Sect B,* 2012, **68**, 1.

10 Z. Zhao, Q. Zeng, H. Zhang, S. Wang, S. Hirai, Z. Zeng, W. L. Mao, *Phys. Rev. B,* 2015, **91**, 184112.

11 I. R. Beattie, K. M. S. Livingston, G. A. Ozin, D. J. Reynolds, *J. Chem. Soc. A: Inorg. Phys. Theore.,* 1970, **3**, 449.

12 N. Cornei, N. Tancret, F. Abraham, O. Mentré, *Inorg. Chem.,* 2006, **45**, 4886.

13 A. Matsumoto, Y. Koyama, I. Tanaka, *Phys. Rev. B,* 2010, **81**, 094117.

14 F. J. Manjón, D. Errandonea, *Phys. Status Solidi B*, 2009, **246**, 9.

15 Y. Zou, X. Qi, X. Wang, T. Chen, X. Li, D. Welch, B. Li, *J. Appl. Phys.,* 2014, **116**, 013516.

16 H.-K. Mao, P. M. Bell, J. W. Shaner, D. J. Steinberg, *J. Appl. Phys.,* 1978, **49,** 3276.

17 A. P. Hammersley, S. O. Svensson, M. Hanfland, A. N. Fitch, D. Hausermann, *High Pressure Res*., 1996, **14,** 235.

18 M. D. Segall, P. L. D. Lindan, M. J. Probert, C. Pickard, P. J. Hasnip, S. J. Clark, M. C. Payne, *J. Phys.: Condens. Matter,* 2012, **14**, 2717.

19 H. J. Monkhorst, J. D. Pack, *Phys. Rev. B,* 1976, **13**, 5188.

20 A.V. D. Walle, G. Ceder, *Phys. Rev. B,* 1999*,* **9,** 14992.

21 Y. Zou, D. He, X. Wei, R. Yu, T. Lu, X. Chang, S. Wang, L. Lei, *Mater. Chem. Phys.,* 2010, **123**, 529.

Table 1. Summary of crystal structure and lattice parameters of Sb_2O_3 polymorphs at various pressures by synchrotron *in situ* x-ray diffraction studies

Structure	*β-Sb₂O₃*	Distorted *β*-phase	New phase
P-T conditions	0.1 MPa, 300 K	8.8 GPa, 300 K	21.3 GPa, 300 K
Crystal structure & Space group	orthorhombic, *Pccn* (No. 56)	distorted-Orth., *Pccn* (No. 56)	monoclinic, *P21/c* (No. 14)
Lattice parameters (Å)	*a* = 4.874 (2) *b* =12.494 (2) *c* = 5.420 (1)	*a* = 4.500 (4) *b* =11.954 (16) *c* = 5.225 (8)	*a* = 4.491 (5) *b* =11.409 (9) *c* =5.119 (5)
Angle (°)	*α*= *β*=*γ*=90	*α*= *β*=*γ*=90	*α*=*γ*=90; *β*= 93.5
Unit-cell volume (Å^3)	333.07(11)	281.1(10)	256.3(34)
Z	4	4	4
Wyckoff sites	Sb1:*8e* (0.044,0.128,0.179) O1: *4c* (0.25, 0.25, -0.075) O2: *8e* (0.147, 0.058, -0.139)		Sb1:*4e* (-0.117,-0.475,0.847) Sb2:*4e* (-0.632,0.051, 0.193) O1: *4c* (-0.25, 0.25, 0.603) O2:*4e* (-0.108, 0.791,0.783) O2:*4e* (-0.608, 0.209,0.001)
R_P, wR_P (%)	1.0, 1.7	1.1, 1.7	0.4, 0.6

Figures and Captions

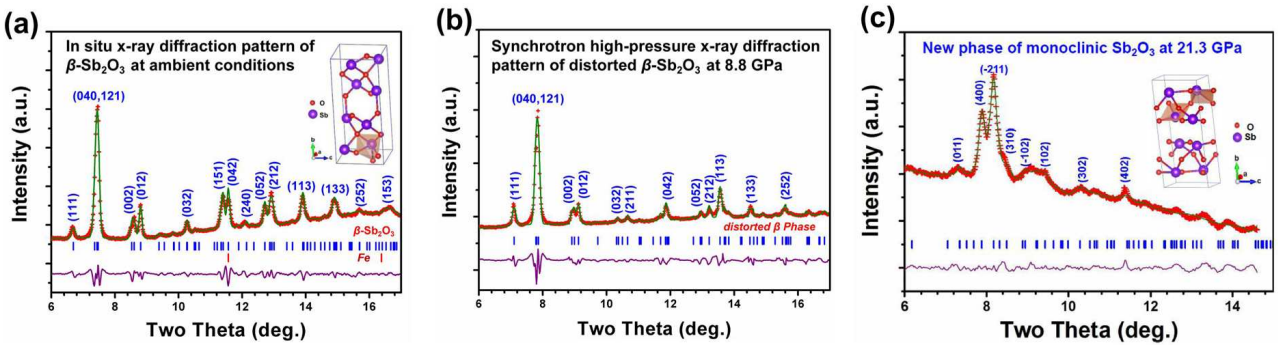

Fig. 1 (a). Synchrotron angle-dispersive x-ray diffraction pattern of the as-prepared β-Sb_2O_3 powder at ambient conditions, suggesting that the as-prepared/starting Sb_2O_3 has an orthorhombic structure (space group: *Pccn*). The crystal structure of valentinite β-Sb_2O_3 is shown as an inset. (b). Representative x-ray diffraction pattern of distorted β-Sb_2O_3 phase upon compression at 8.8 GPa and 300 K. (c). *In situ* x-ray diffraction pattern of the new discovery of monoclinic Sb_2O_3 phase at ~21. 3 GPa and 300 K, and its crystal structure is shown as an inset. The tick marks correspond to the peak positions of the orthorhombic β-Sb_2O_3 (PDF: #11-0689), the new monoclinic Sb_2O_3, and the cubic Fe from the iron gasket used in our diamond-anvil-cell experiments.

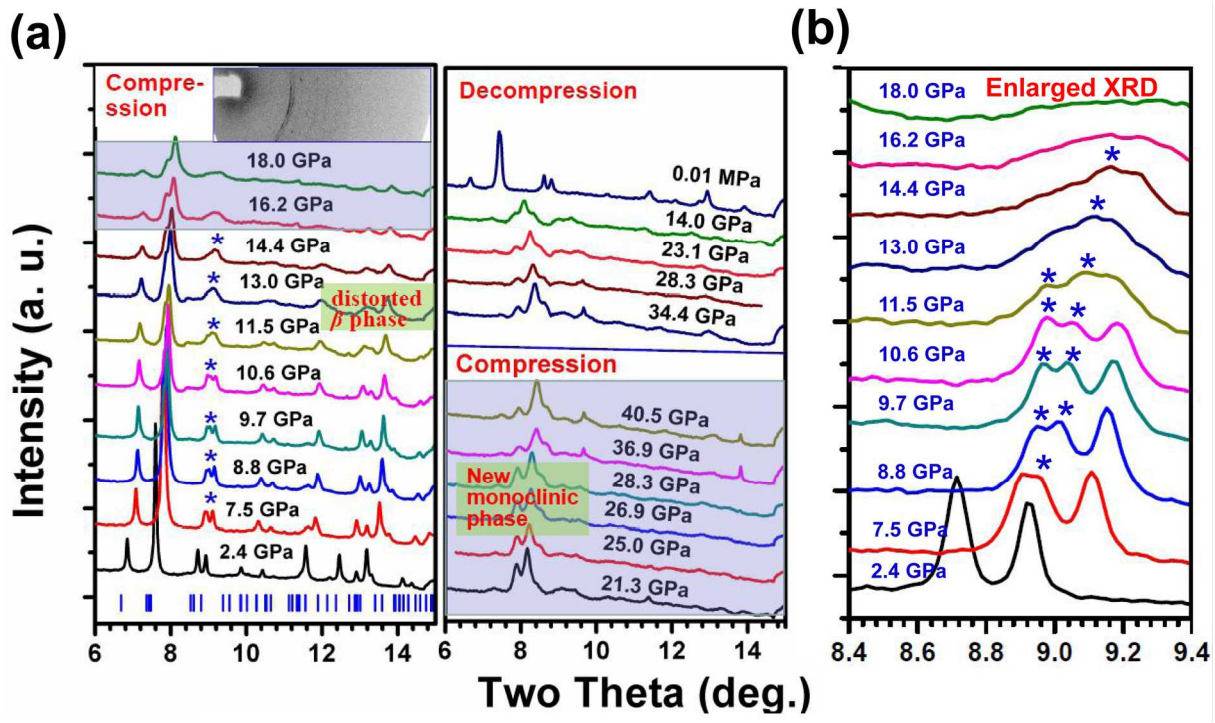

Fig. 2 (a). Selected synchrotron angle-dispersive x-ray diffraction patterns of β-Sb_2O_3 upon compression up to ~40.5 GPa, in comparison with those during decompression (top panel). A representative two-dimensional XRD image at ~40.5 GPa is shown as an inset, indicating an amorphous component of Sb_2O_3 polymorph. The tick marks corresponded to the peak positions of the orthorhombic β-Sb_2O_3 (PDF: #11-0689) are shown below. The blue asterisk symbolizes the split peaks of (121, 040, 012) as induced by structural distortions; The shallow area indicates the formation of a new monoclinic Sb_2O_3 phase; (b). Enlarged x-ray diffraction patterns of β-Sb_2O_3 upon compression at pressures ranging from 2.4 to 18.0 GPa (for split peaks), indicating the occurrence of isostructural distortion transition in Sb_2O_3 sample.

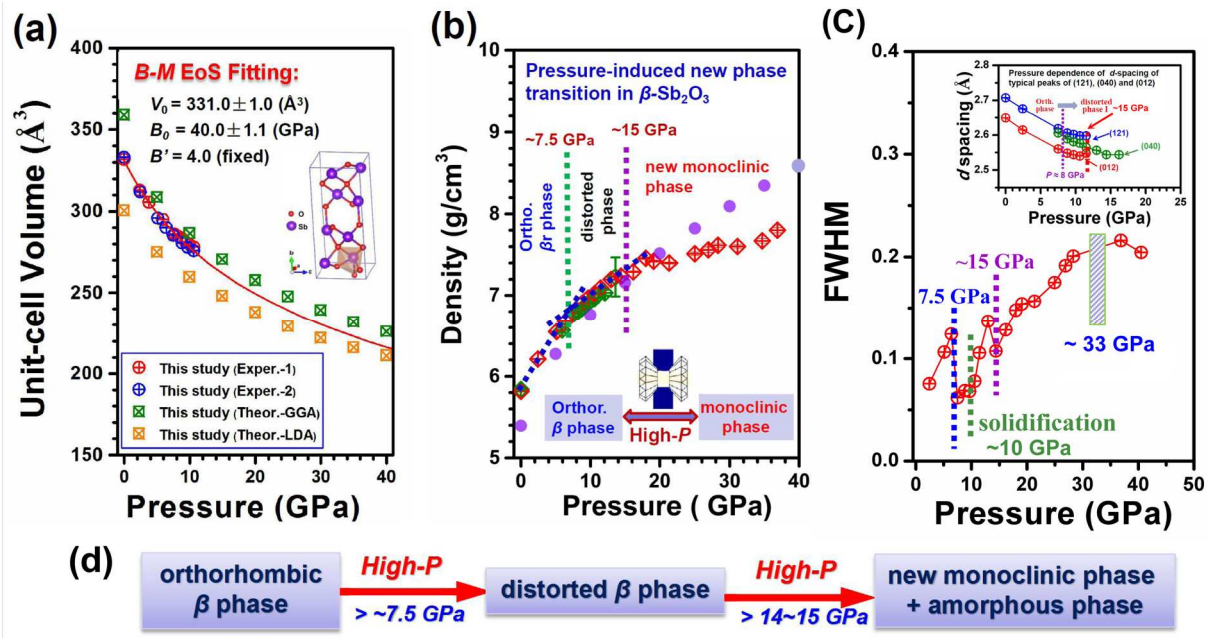

Fig. 3 (a). *P-V* relations in β-Sb_2O_3 valentinite at room temperature obtained from the current synchrotron x-ray diffraction experiments (blue and red circles), in comparison with our theoretical results from first-principles calculations (green and orange squares). The red curve shows the fitting results of the current experimental study using second-order Birch-Mürnaghan equation of state, giving B_0 = 40.0 ± 1.1 GPa, V_0 = 331.0 ± 1.0 Å^3 with B' = 4.0 (fixed). (b). Density changes of Sb_2O_3 polymorphs at high pressure determined from the current *in situ* x-ray diffraction measurements (green and red squares), compared with our theoretical calculations (purple circles: GGA). (c). A representative XRD FWHM (full width at half maximum) pattern for (121/040) peak (symbolized as red circles) of β-Sb_2O_3 as a function of pressure, showing a pronounced pressure-induced discontinuity at ~7.5 GPa. (d). Pathways of the phase transformations in β-Sb_2O_3 under high pressure.

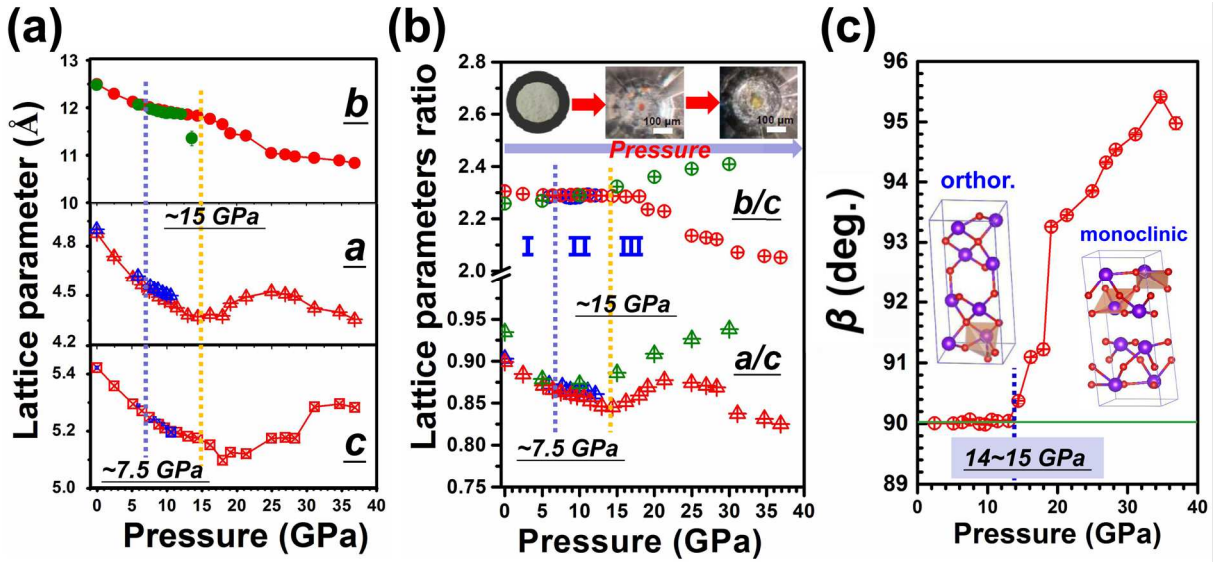

Fig. 4. (a). Experimental lattice parameters (*a, b* and *c*) of Sb_2O_3 polymorphs at high pressure derived from the current synchrotron x-ray diffraction measurements (green circles and blue symbols for Run 1; red symbols for Run 2). (b). Experimental lattice ratios for *b/c* and *a/c* for Sb_2O_3 at high pressure from the current x-ray diffraction measurements (blue and red symbols for Run 1 and 2), in comparison with our first-principles theoretical results (green symbols). The optical photographs of the sample are shown as insets, indicating the phase-transition-induced color changes in Sb_2O_3 upon compression. (c). The angle β between the *a* and *c* axes determined from the refinement of our synchrotron x-ray diffraction of Sb_2O_3 at high-*P* (red circles), indicating a pronounced distorted-orthorhombic-to-monoclinic phase transition in Sb_2O_3 occurred upon compression at pressures above 14~15 GPa.

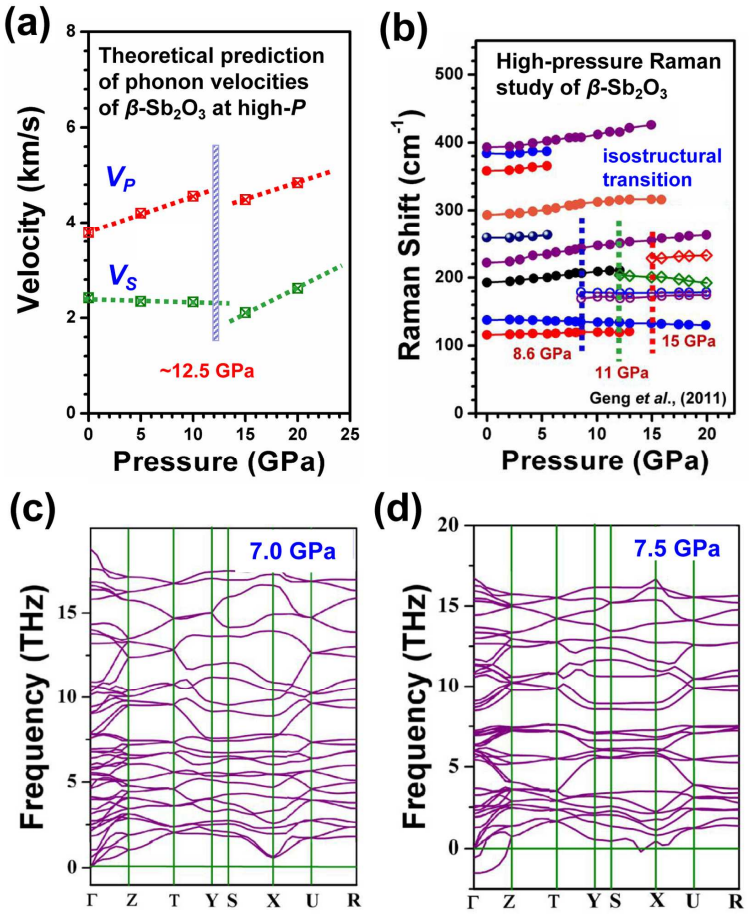

Fig. 5 (a) Acoustic/Phonon velocities of β-Sb_2O_3 as a function of pressure derived from the current first-principles calculations of elastic constants (green and red squares). The predicted discontinuity at ~12.5 GPa indicates the structural instability of β-Sb_2O_3 at high pressure. (b) High-pressure Raman study on β-Sb_2O_3, suggesting an isostructural phase transitions from the orthorhombic structure to a new phase occurred at 8.6~15 GPa by Geng *et al.*[2] (c) Phonon dispersion curves of orthorhombic β-Sb_2O_3 at typical pressures of 7.0 GPa and (d) 7.5 GPa. The imagery phonon vibration modes at 7.5 GPa indicates that the orthorhombic β-Sb_2O_3 phase becomes dynamically unstable at pressures above 7.5 GPa, supporting our experimental results that isostructural distortion transition occurred at ~7.5 GPa. The coordinates of the high symmetry *k*-points are shown as: Γ(0, 0, 0), Z (0, 0, 0.5), T (-0.5, 0, 0.5), Y (-0.5, 0, 0), S (-0.5, 0.5, 0), X (0, 0.5, 0), U (0, 0.5, 0.5), R (-0.5, 0.5, 0.5).

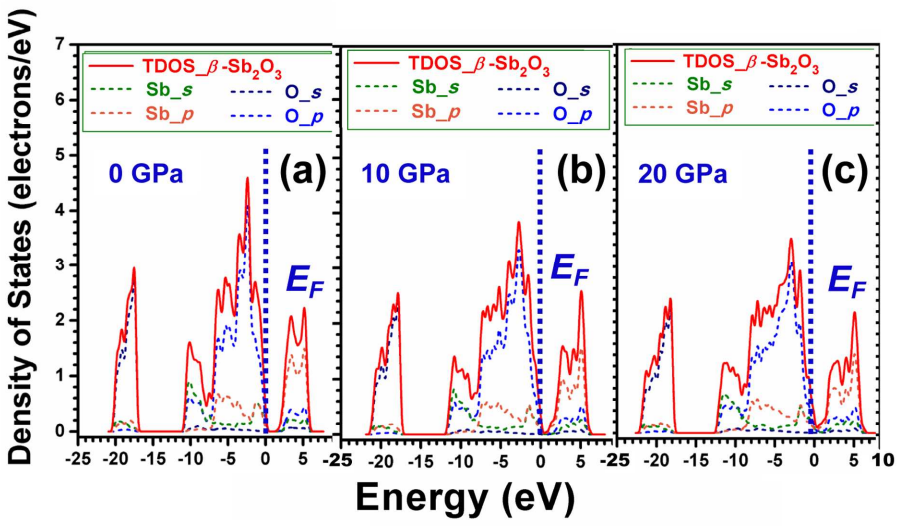

Fig. 6. (a). Calculated total and partial density of states of the orthorhombic β-Sb_2O_3 at 0 GPa, in comparison with those at (b) 10 GPa and (c) 20 GPa.